Hindawi
Journal of Sensors
Volume 2020, Article ID 8811448, 8 pages
https://doi.org/10.1155/2020/8811448

Research Article

Active Vibration Control of PID Based on Receptance Method

Lijuan Peng,[1] Jian Wang,[2] Guicheng Yu,[3] Zuoxue Wang,[2] Aijun Yin,[2] and Hongji Ren[2]

[1]*Department of Computer Science and Technology, Southwest University of Science and Technology, Mianyang 621010, China*
[2]*College of Mechanical Engineering, Chongqing University, Chongqing 400044, China*
[3]*Gas Storage Management Department, PetroChina Southwest Oil & Gas Field Company, Chongqing 401147, China*

Correspondence should be addressed to Jian Wang; vi@cqu.edu.cn

Received 19 June 2020; Revised 10 July 2020; Accepted 10 July 2020; Published 14 August 2020

Academic Editor: Bin Gao

Active vibration control approaches have been widely applied on improving reliability of robotic systems. For linear vibratory systems, the vibration features can be altered by modifying poles and zeros. To realize the arbitrary assignment of the closed-loop system poles and zeros of a linear vibratory system, in this paper, an active PID input feedback vibration control method is proposed based on the receptance method. The establishment and verification of the proposed method are demonstrated. The assignable poles during feedback control are calculated and attached with importance to expand the application of the integral control. Numerical simulations are conducted to verify the validity of the proposed method in terms of the assignment of closed-loop poles, zeros, and both. The results indicate that the proposed method can be used to realize the active vibration control of closed-loop system and obtain the desired damping ratio, modal frequency, and dynamic response.

1. Introduction

Nowadays, the demand for lower vibration and higher reliability in robotic systems is increasing [1]. Extensive studies have been conducted to optimize the controlling of various nonlinear systems [2–6]. A common vibration control approach is to modify system dynamics using controllers [7]. PID-based approaches have been widely applied on motion control of robotic systems [8, 9]. Generally, the vibration characteristics of a linear vibratory system are determined by its zeros and poles, and the assignment of eigenvalues in a system is of great importance in improving system reliability.

Traditionally, the solutions of pole assignment are solved by using the information of mass, damping, and stiffness matrices acquired from the finite element (FE) models [10]. However, FE models are generally limited by the incapability in obtaining precise damping models of real structures. Ram and Mottershead [11] developed an active vibration control method for linear system based on receptance method to accurately assign the system poles and zeros to specified values. One considerable advantage of this method is that it is entirely based on data from modal testing rather than the exact mass, damping, and stiffness matrices. Mottershead et al. assigned part of the system poles to the predetermined values while keeping nonimportant poles unchanged by making the nonimportant poles uncontrollable or unobservable [12]. Zhang et al. presented the theory of applying acceleration feedback and position feedback to the nondamping system to assign part of poles [13]. Ouyang proposed a method of using acceleration feedback and velocity feedback in active vibration control [14]. Recently, neural network- (NN-) based pole-zero assignment methods have gained a lot of attention [15–18]. However, NN-based approaches may fail to yield desired results on practice due to the black-box nature of NN and the requirement of NN parameter optimization skills.

Previous studies indicate that various combinations of acceleration, velocity, and position make it flexible and applicable to select the type of feedback when implementing active vibration control. However, a vibration system will inevitably become a singular system when the acceleration feedback is applied, which leads to the unavailability of the receptance method. In this paper, integral control is introduced to overcome this limitation. The contributions of this paper are summarized as follows: (1) A PID input feedback active vibration control method is proposed based on the receptance method. (2) The numerical solutions for assignment

of closed-loop poles and zeros by applying the proposed method are demonstrated.

The rest of the paper is organized as follows: The assignments of poles and zeros in PID control systems are demonstrated in Section 2 and Section 3, respectively. Then, numerical simulations are conducted to verify the validity of the proposed method in Section 4. Finally, Section 5 concludes the paper.

2. Pole Assignment of PID Control Systems

2.1. Formulation of Pole Assignment. The equation of a n degree freedom linear system can be described in second-order form as follows according to [19]:

$$M\ddot{x}(t) + C\dot{x}(t) + Kx(t) = 0, \tag{1}$$

where $M, C, K \in R^{n\times n}$ are mass, damping, and stiffness matrices, respectively; $x(t) \in R^{n\times 1}$ is the displacement vector. $M = M^{\mathrm{T}}, C = C^{\mathrm{T}}, K = K^{\mathrm{T}}$, and for any nonzero vector $v \in R^{n\times 1}$, there is $v^{\mathrm{T}}Mv \geq 0$, $v^{\mathrm{T}}Cv \geq 0$, and $v^{\mathrm{T}}Kv \geq 0$.

Integrate PID feedback control to the system and the closed-loop system can be written as follows:

$$M\ddot{x}(t) + C\dot{x}(t) + Kx(t) = bu(t), \tag{2}$$

where $b \in R^{n\times 1}$ is the force distribution vector and $u(t)$ is the input control vector:

$$u(t) = g_1^{\mathrm{T}}x(t) + g_2^{\mathrm{T}}\int_0^t x(\tau)d\tau + g_3^{\mathrm{T}}\dot{x}(t), \tag{3}$$

where $g_1, g_2, g_3 \in R^{n\times 1}$ are input control gain vectors for displacement, differential, and velocity, respectively.

Express Equation (2) in the Laplace space:

$$\left[Ms^2 + Cs + K\right]x(s) = b\left(g_1^{\mathrm{T}} + \frac{g_2^{\mathrm{T}}}{s} + sg_3^{\mathrm{T}}\right)x(s). \tag{4}$$

Then,

$$\left[Ms^2 + Cs + K - b\left(g_1^{\mathrm{T}} + \frac{g_2^{\mathrm{T}}}{s} + sg_3^{\mathrm{T}}\right)\right]x(s) = 0. \tag{5}$$

Equation (5) shows that the highest order of the system stiffness matrix is a positive definite matrix, so the closed-loop system must be a nonsingular system. Therefore, the system receptance matrix exists.

The receptance matrix can be obtained by applying the Sherman–Morrison formula for Equation (5):

$$\widehat{H}(s) = H(s) + \frac{H(s)b(g_1 + (g_2/s) + sg_3)^{\mathrm{T}}H(s)}{1 - (g_1 + (g_2/s) + sg_3)^{\mathrm{T}}H(s)b}, \tag{6}$$

where $H(s) = [Ms^2 + Cs + K]^{-1}$ is the receptance matrix of the open-loop system, which can be obtained in practice by measuring the receptance $H(i\omega)$ [20]. The characteristic polynomial $p(s)$ can be derived from Equation (6) at the same time:

$$p(s) = 1 - \left(g_1 + \frac{g_2}{s} + sg_3\right)^{\mathrm{T}}H(s)b. \tag{7}$$

Thus, the roots of Equation (8) are the pole of the closed-loop system:

$$p(s) = 0. \tag{8}$$

Given $H(s)$, b, and Equation (9):

$$p(\mu_i) = 0. \tag{9}$$

The problem of assigning the poles of a closed-loop system to setpoints $\{\mu_1, \mu_2, \cdots, \mu_N\}$ can be transformed to the solution of input control gain vectors g_1, g_2, and g_3. Where $\mu_i \in \{\mu_i\}_{i=1}^N$, $\mu_i \neq 0$, $\{\mu_i\}_{i=1}^N$ is closed under conjugation, N is the number of closed-loop system poles that can be assigned.

2.2. Minimum Number of Assignable Poles N. Given a positive definite system with closed-loop conjugate poles $\{\mu_i\}_{i=1}^N$, suppose that the adjoint matrix of $H(s)$ is $A(s)$ and the determinant is $D(s)$. $p(s) = 0$ can be expressed as follows:

$$1 - \left(g_1 + \frac{g_2}{s} + sg_3\right)^{\mathrm{T}}\frac{A(s)}{D(s)}b = 0. \tag{10}$$

Since for any $\mu_i \in \{\mu_i\}_{i=1}^N$, $D(\mu_i) \neq 0$, Equation (10) can be written as follows:

$$sD(s) - \left(sg_1 + g_2 + s^2g_3\right)^{\mathrm{T}}A(s)b = 0. \tag{11}$$

Set

$$q(s) = \left(sg_1 + g_2 + s^2g_3\right)^{\mathrm{T}}A(s)b. \tag{12}$$

The highest degree of s in $q(s)$ is $(2n-2)+2 = 2n$ and the highest degree of s in $D(s)$ is $2n$. Since the number of closed-loop poles N is equal to the degree of Equation (10) and the highest degree of s in Equation (10) is $2n+1$, the number of characteristic polynomial root is $N = 2n+1$. It should be noted that due to the introduction of integral control, the closed-loop system will produce an extra nonzero pole.

In fact, the introduction of integral control into closed-loop system will lead to a nonregular and generalized system. The closed-loop system is stable if (1) it is regular and (2) all of its assigned poles have negative real components [21]. The regularity of the closed-loop system in this method is guaranteed by the positive definiteness of the mass matrix. The values of the assigned poles can be arranged to stabilize the closed-loop system given that their real components are negative and $\{\mu_i\}_{i=1}^N$ is self-conjugate.

2.3. Calculate Vectors g_1, g_2, g_3 and Minimum Sensor Layout Method. The solution of g_1, g_2, g_3 can be realized by the following equation:

$$Gg = \gamma, \tag{13}$$

where

$$G = \begin{bmatrix} \Psi_1^{\mathrm{T}} & \dfrac{\Psi_1^{\mathrm{T}}}{\mu_1} & \mu_1\Psi_1^{\mathrm{T}} \\ \Psi_2^{\mathrm{T}} & \dfrac{\Psi_2^{\mathrm{T}}}{\mu_2} & \mu_2\Psi_2^{\mathrm{T}} \\ & \vdots & \\ \Psi_N^{\mathrm{T}} & \dfrac{\Psi_N^{\mathrm{T}}}{\mu_N} & \mu_N\Psi_N^{\mathrm{T}} \end{bmatrix}, \Psi_i = H(\mu_i)b,$$
$$g^{\mathrm{T}} = \begin{bmatrix} g_1^{\mathrm{T}} & g_2^{\mathrm{T}} & g_3^{\mathrm{T}} \end{bmatrix} \tag{14}$$
$$\gamma^{\mathrm{T}} = [1\ 1 \cdots 1]$$

and $G \in R^{N\times 3n}$, $g \in R^{3n\times 1}$, and $\gamma \in R^{N\times 1}$.

The pole assignment problem raised by Equation (2) can be solved by applying Equation (13) and Equation (14). One solution for Equation (13) is as follows:

$$g = G^{+}\gamma, \tag{15}$$

where G^{+} is the Moore–Penrose generalized inverse of G. When the assigned closed-loop poles are self-conjugate, g_1, g_2, and g_3 can be calculated according to Equations (13)–(15).

Considering the limitation of the additional mass in the actual control system, the number of sensors used to measure the motion parameters of the system should be as small as possible. Therefore, the value of some items in g_1, g_2, g_3 can be assigned to zero by setting the values of the corresponding columns of the G to be zero. In practice, the solution means that fewer sensors are involved. Due to the integration of PID input feedback control and $N = 2n + 1$, the number that can be allocated to zero in G has at most 3 $n - N = n - 1$ columns. Therefore, the number of sensors can be reduced accordingly in practice to minimize the effect of the additional mass on the system.

2.4. Validity Analysis. When the value of the preset poles $\{\mu_i\}_{i=1}^{N}$ and the optional $k\,(0 \le k \le n-1)$ column vector to be replaced by the 0 in the G are determined, a specific PID input feedback solution is derived, identified as W_k. From Equations (13)–(15), g_1, g_2, g_3 can be calculated in this specific PID input feedback solution. Below we will show how to verify whether W_k is valid or not.

The closed-loop receptance matrix $\widehat{H}(s)$ can be derived from Equation (5) as follows:

$$\widehat{H}(s) = \Omega(s)^{-1}, \tag{16}$$

where $\Omega(s)$ is as follows:

$$\Omega(s) = Ms^2 + Cs + K - b\left(g_1^{\mathrm{T}} + \frac{g_2^{\mathrm{T}}}{s} + sg_3^{\mathrm{T}}\right). \tag{17}$$

The problem of verifying whether a particular W_k is valid is equivalent to verifying whether $\Omega(s)$ is a nonsingular matrix for any $s \notin \{\mu_i\}_{i=1}^{N}$ under the determined case. The verification process of W_k is as follows: Firstly, the real vectors g_1, g_2, g_3 are calculated according to Equations (13)–(15). Then, substitute g_1, g_2, g_3 into Equation (17) and obtain the determinant $w(s)$ of $\Omega(s)$. For any $s \notin \{\mu_i\}_{i=1}^{N}$, if $w(s)$ is zero, the closed-loop system poles cannot be assigned to the designated values, meaning that W_k is invalid. Otherwise, the closed-loop system poles can be assigned to the specified desired values, indicating that W_k is valid.

3. Zero Assignment of PID Control Systems

3.1. Formulation of Zero Assignment. The characteristic polynomial for the zeros of receptance $\widehat{H}_{ij}$ can be realized when the denominator matrix (i, j) of Equation (6) is zero:

$$\widehat{H}_{ij}(s) = e_i^{\mathrm{T}}\left(H(s) + \frac{H(s)b(g_1 + (g_2/s) + sg_3)^{\mathrm{T}}H(s)}{1 - (g_1 + (g_2/s) + sg_3)^{\mathrm{T}}H(s)b}\right)e_j, \tag{18}$$

where e_i, e_j are the unit vectors obtained from the corresponding columns of the identity matrix.

Therefore, the problem of assigning zeros of the closed-loop system receptance $\widehat{H}_{ij}$ to the setpoints $\{\xi_1, \xi_1, \cdots, \xi_r\}$ can be realized as follows:

Given $H(s)$, b, i, j, and

$$e_i^{\mathrm{T}}\left\{\left[1 - \left(g_1 + \frac{g_2}{\xi_k} + \xi_k g_3\right)^{\mathrm{T}}H(\xi_k)b + H(\xi_k)b\left(g_1 + \frac{g_2}{\xi_k} + \xi_k g_3\right)^{\mathrm{T}}\right]H(\xi_k)\right\}e_j = 0 \tag{19}$$

Calculate the input control gain vectors g_1, g_2, g_3. Where $\xi_k \notin \{\xi_i\}_{i=1}^{r}$, $r \le 2n - 1$, r is the number of poles in a closed-loop system that can be assigned.

Equation (19) can be written in the following form:

$$H_{ij}(\xi_k)\left[\left(g_1 + \frac{g_2}{\xi_k} + \xi_k g_3\right)^{\mathrm{T}}H(\xi_k)b\right] - e_i^{\mathrm{T}}H(\xi_k)b\left(g_1 + \frac{g_2}{\xi_k} + \xi_k g_3\right)^{\mathrm{T}}H(\xi_k)e_j = H_{ij}(\xi_k), \tag{20}$$

where $H_{ij}(s)$ is the open-loop receptance value at the open-loop system coordinate of (i, j). Transform Equation

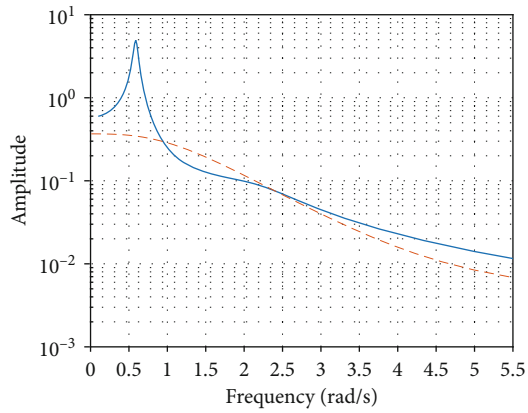

FIGURE 1: The frequency response for the original system $H_{3,3}$ (solid line) and the modified system $H_{3,3}$ (dotted line).

(20) to $(g_1 + (g_2/\xi_k) + \xi_k g_3)^{\mathrm{T}}(H_{ij}(\xi_k)H(\xi_k)b - e_i^{\mathrm{T}}H(\xi_k)bH(\xi_k)e_j) = H_{ij}(\xi_k)$. Since $e_i^{\mathrm{T}}H(\xi_k)b$ is a scalar, set

$$t_k = H_{ij}(\xi_k)H(\xi_k)b - e_i^{\mathrm{T}}H(\xi_k)bH(\xi_k)e_j. \tag{21}$$

We have $(g_1 + (g_2/\xi_k) + \xi_k g_3)^{\mathrm{T}} t_k = H_{ij}(\xi_k)$. Since $H_{ij}(\xi_k)$ is scalar, after transposing we get $t_k^{\mathrm{T}} g_1 + (t_k^{\mathrm{T}} g_2/\xi_k) + \xi_k t_k^{\mathrm{T}} g_3 = H_{ij}(\xi_k)$, i.e., $\begin{pmatrix} t_k^{\mathrm{T}} & t_k^{\mathrm{T}}/\xi_k & \xi_k t_k^{\mathrm{T}} \end{pmatrix} \begin{pmatrix} g_1 \\ g_2 \\ g_3 \end{pmatrix} = H_{ij}(\xi_k)$. Therefore, for preset closed-loop system zeros $\{\xi_1, \xi_1, \cdots, \xi_r\}$, we have

$$T \begin{pmatrix} g_1 \\ g_2 \\ g_3 \end{pmatrix} = \begin{pmatrix} H_{ij}(\xi_1) \\ H_{ij}(\xi_2) \\ \vdots \\ H_{ij}(\xi_r) \end{pmatrix}, \tag{22}$$

where

$$T = \begin{bmatrix} t_1^{\mathrm{T}} & \dfrac{t_1^{\mathrm{T}}}{\mu_1} & t_1^{\mathrm{T}}\xi_1 \\ t_2^{\mathrm{T}} & \dfrac{t_2^{\mathrm{T}}}{\mu_2} & t_2^{\mathrm{T}}\xi_2 \\ & \vdots & \\ t_r^{\mathrm{T}} & \dfrac{t_r^{\mathrm{T}}}{\mu_r} & t_r^{\mathrm{T}}\xi_r \end{bmatrix}. \tag{23}$$

It can be seen from Equation (22) that the inverse of the matrix T can be obtained when the preset zeros $\{\xi_1, \xi_1, \cdots, \xi_r\}$ are given, and then the real vectors g_1, g_2, g_3 can also be obtained. In particular, when i and j are overlapped, the distribution of zeros will affect the closed-loop pole assignment of the system, which is significant [22].

3.2. Pole and Zero Assignment. We can assign the zeros and poles in the closed-loop system at the same time according to Equation (13) and Equation (22). In this case, the total number of zeros and poles follows $r + N \le 2n + 1$. Similarly, by assigning $k\,(0 \le k \le n-1)$ columns in Equation (13) and Equation (22) to zero, we can get the optimized allocation scheme.

4. Numerical Simulations

4.1. Pole Assignment Simulation. Consider a three-degree-of-freedom system with matrices:

$$M = \begin{bmatrix} 2 & & \\ & 2 & \\ & & 3 \end{bmatrix},$$
$$C = \begin{bmatrix} 2.5 & -2 & 0 \\ -2 & 3 & -1 \\ 0 & -1 & 1 \end{bmatrix}, \tag{24}$$
$$K = \begin{bmatrix} 10 & -3 & -4 \\ -3 & 3 & 0 \\ -4 & 0 & 4 \end{bmatrix}.$$

The open-loop poles are $-0.0305 \pm 0.5894i$, $-0.8503 \pm 1.0119i$, and $-0.6609 \pm 2.1200i$.

Now use pole assignment method proposed in this paper to modify the closed-loop response of the system. Set $b = [1 \quad 1 \quad 1]^{\mathrm{T}}$. For $n = 3$, $N = 7$ according to Section 2.2. Since the original system has a lower characteristic frequency and a smaller damping ratio, the closed-loop system characteristic values ate assigned as $\mu_{1;2} = -1 \pm 0.5i$, $\mu_{3;4} = -1 \pm i$, $\mu_{5;6} = -2 \pm i$, and $\mu_7 = -3$ to increase the damping of the system and enhance the stability.

Obtain g_1, g_2, g_3 according to Equations (13)–(15):

$$\begin{cases} g_1 = [-38.1817 \quad -6.7810 \quad 11.3765]^{\mathrm{T}}, \\ g_2 = [3.7396 \quad -14.4487 \quad 2.4203]^{\mathrm{T}}, \\ g_3 = [-4.1357 \quad -4.5904 \quad -10.6608]^{\mathrm{T}}. \end{cases} \tag{25}$$

The above PID input feedback solution is valid according to Section 2.4. In order to visualize the effect of this method, the frequency response curve, zero-pole distribution, and Nyquist plot of the $H_{3,3}$ of original system and the modified system are given, shown in Figures 1–5. Figures 2 and 3 show that the poles of the modified system are assigned to the specified positions, and an additional pole is added to the modified system due to the integration of integral feedback. The introduction of the extra pole improves the flexibility to handle the closed-loop systems in engineering applications. We can see from Figure 1, Figure 4, and Figure 5 that after pole

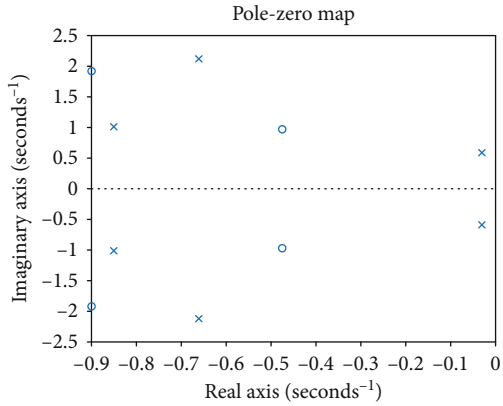

Figure 2: The zero-pole map for the original system $H_{3,3}$.

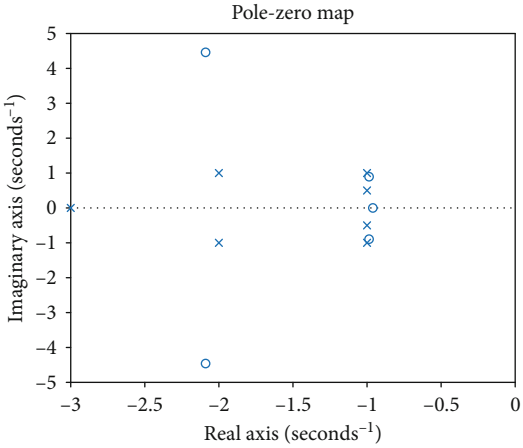

Figure 3: The zero-pole map for the modified system $H_{3,3}$.

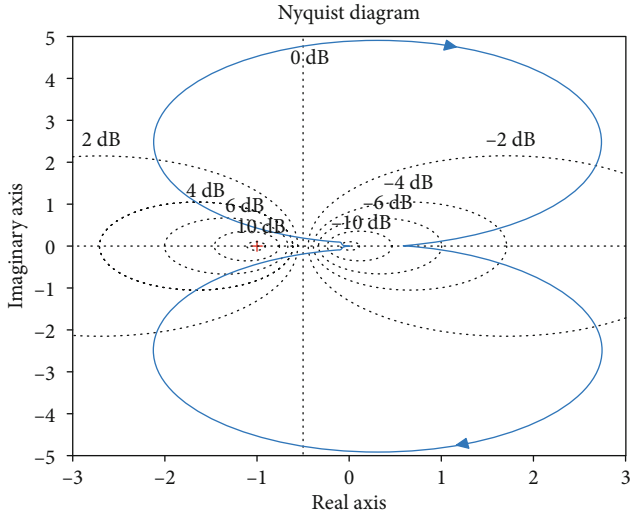

Figure 4: The Nyquist curve for the original system $H_{3,3}$.

reassignment, system features such characteristic frequency, damping, and stability have been changed, and the overall performances have been improved.

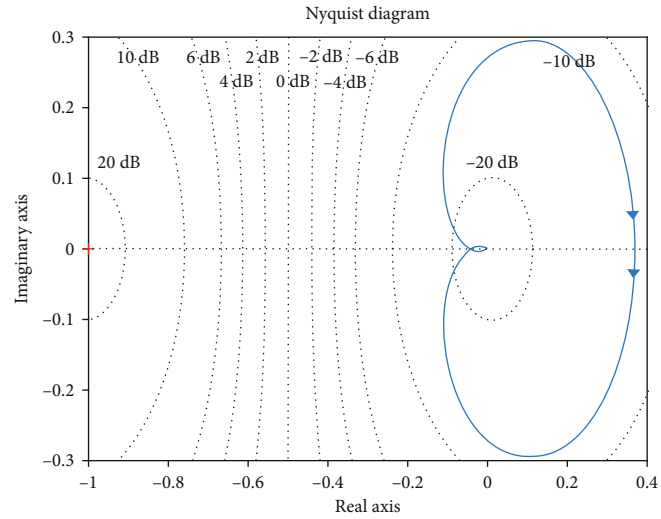

Figure 5: The Nyquist curve for the modified system $H_{3,3}$.

Table 1: Pole assignment solutions.

Plan	Column replaced by a zero vector in G
W_1	{1}, {2}, {3}, {4}, {5}, {6}, {7}, {8}, {9}
W_2	{1,2}, {1,3}, {2,3}, {1,4}, {2,4}, {3,4}, {1,5}, {2,5}, {3,5}, {4,5}, {1,6}, {2,6} {3,6}, {4,6}, {5,6}, {1,7}, {2,7}, {3,7}, {4,7}, {5,7}, {6,7}, {1,8}, {2,8}, {3,8}, {4,8}, {5,8}, {6,8}, {7,8}, {1,9}, {2,9}, {3,9}, {4,9}, {5,9}, {6,9}, {7,9}, {8,9}

Table 2: The control gains that correspond to Table 1.

Plan	Control gain
W_1	$g_1 = [0 \quad -64.6499 \quad 33.3755]^T$
	$g_2 = [55.1590 \quad -68.2535 \quad 18.7660]^T$
	$g_3 = [5.1115 \quad -31.2131 \quad 15.4023]^T$
W_2	$g_1 = [0 \quad 0 \quad -23.1931]^T$
	$g_2 = [301.6367 \quad -56.1317 \quad -191.4356]^T$
	$g_3 = [37.4365 \quad 9.1931 \quad -93.6944]^T$

4.2. Minimum Sensor Configuration for Pole Assignment. Based on the pole assignment in Section 4.1 and the minimum sensor layout in Section 2.3, a minimum sensor configuration scheme for pole assignment simulation is developed and verified according to Section 2.4. Table 1 shows all solutions that can assign the poles of the closed-loop system to preset values $\mu_{1;2} = -1 \pm 0.5i$, $\mu_{3;4} = -1 \pm i$, and $\mu_{5;6} = -2 \pm i$, while keeping the closed-loop system stable at the same time for the case in Section 4.1. The PID feedback gains for the 2 solutions are given in Table 2 (only the control gains of the first method in each W_k are given). The system performance may destabilize when the number of assigned poles is less than N (i.e., when the lacked poles are assigned, the number of assigned poles in Table 3 is $2n$). This highlights the importance of determining the number of assignments. The specific results are demonstrated in Tables 1–3.

Table 3: Results under lacked poles.

Preset poles	Control gain	Actual poles
$\{\mu_i\}_{i=1}^{2n} = \begin{Bmatrix} -1 \pm 0.5i \\ -1 \pm i \\ -2 \pm i \end{Bmatrix}$	$g_1 = [-8.8455 \quad 0.9987 \quad -11.5646]^{\mathrm{T}}$ $g_2 = [4.9075 \quad 1.1948 \quad -1.5619]^{\mathrm{T}}$ $g_3 = [-13.0963 \quad 1.7248 \quad 5.5819]^{\mathrm{T}}$	$\begin{Bmatrix} -1 \pm 0.5i \\ -1 \pm i \\ -2 \pm i \\ 1.0915 \end{Bmatrix}$

4.3. Zero Assignment Simulation. Considering the three-degree-of-freedom system in Section 4.1, we use zero assignment method in Section 3 to modify the closed-loop system zeros and the closed-loop response of the system.

Set $b = [1 \quad 1 \quad 1]^{\mathrm{T}}$ and the closed-loop system $H_{3,3}(s)$ zeros as $\xi_{1;2} = -1 \pm 0.5\mathrm{i}$, $\xi_{3;4} = -2 \pm 0.5i$. Obtain g_1, g_2, g_3 according to Equation (22):

$$\begin{cases} g_1 = [1.9623 \quad -3.0448 \quad 0]^{\mathrm{T}}, \\ g_2 = [-1.3215 \quad -0.4912 \quad 0]^{\mathrm{T}}, \\ g_3 = [-6.3791 \quad -1.4682 \quad 0]^{\mathrm{T}}. \end{cases} \tag{26}$$

The closed-loop poles calculated are $-0.1439 \pm 0.5047i$, $-0.6195 \pm 1.6824i$, $-1.0199 \pm 0.9522i$, and -3.4404. The poles are distributed in the left half plane of the imaginary axis and the closed-loop system is stable. The frequency response curve, the zero-pole distribution diagram, and the Nyquist diagram of the modified system $H_{3,3}$ are illustrated in Figure 6, Figure 7, and Figure 8, respectively. Comparing Figure 2 with Figure 7, we can see that the zeros of the system are accurately assigned to the desired values. Figure 4, Figure 6, and Figure 8 indicate that, after the assignment of zeros, the system stability increases.

4.4. Pole and Zero Assignment Simulation. Based on the three-degree-of-freedom system in Section 4.1, set $b = [1 \quad 1 \quad 1]^{\mathrm{T}}$, the closed-loop system $H_{3,3}(s)$ zeros as $\xi_{1;2} = -1 \pm 0.5i$, and the closed-loop system poles as $\mu_{1;2} = -1 \pm 0.5i$. Obtain g_1, g_2, g_3 according to Equations (13)–(15) and Equation (22):

$$\begin{cases} g_1 = [1.9623 \quad -3.0448 \quad 0]^{\mathrm{T}}, \\ g_2 = [-1.3215 \quad -0.4912 \quad 0]^{\mathrm{T}}, \\ g_3 = [-6.3791 \quad -1.4682 \quad 0]^{\mathrm{T}}. \end{cases} \tag{27}$$

The closed-loop poles calculated at this time are $-0.3563 \pm 1.6213i$, $-0.9778 \pm 0.9769i$, $-1 \pm 0.5i$, and -3. The poles are distributed in the left half plane of the imaginary axis and the closed-loop system is stable. The frequency response curve, the zero-pole distribution diagram, and the Nyquist diagram of the modified system $H_{3,3}$ are illustrated in Figure 9, Figure 10, and Figure 11, respectively. Figure 2 and Figure 10 indicate that the system zeros and poles are accurately assigned to the desired values. After the assignment, an increased system stability is observed according to Figure 4, Figure 9, and Figure 11. The validity of the proposed method is verified by the simulation results.

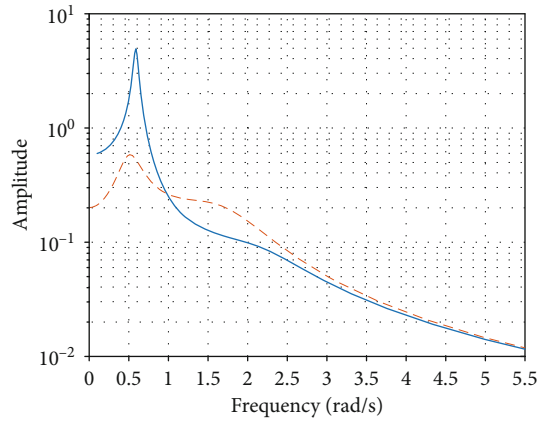

Figure 6: The frequency response for the original system $H_{3,3}$ (solid line) and the modified system $H_{3,3}$ (dotted line).

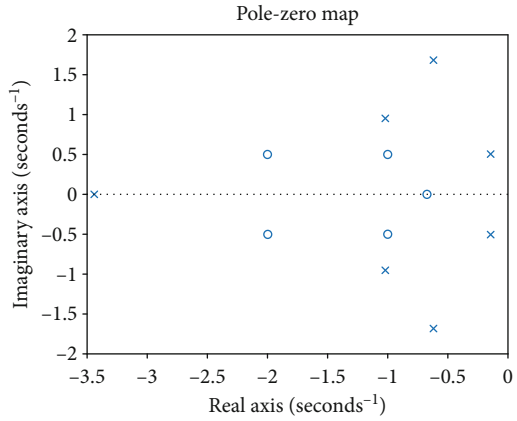

Figure 7: The pole-zero map for the modified system $H_{3,3}$.

5. Conclusions

In this paper, a PID-active vibration control method is proposed based on the receptance method. The proposed method can be utilized to assign the poles and zeros of closed-loop systems in order to improve the performances. Due to the integration of integral control, the proposed method guarantees the positive definiteness of the system and avoids the appearance of a nonsingular system. The proposed method also extends the application of the dynamic flexibility method. The procedures of assigning poles and zeros to a system are demonstrated. Numerical simulations for pole and zero assignments are conducted. Simulation

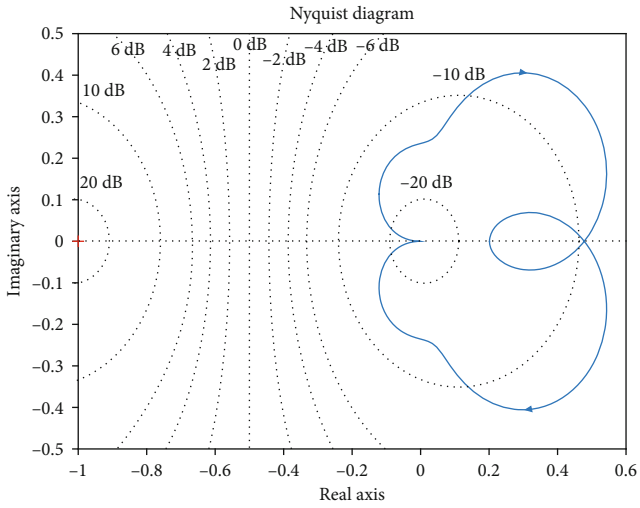

Figure 8: The Nyquist curve for the modified system $H_{3,3}$.

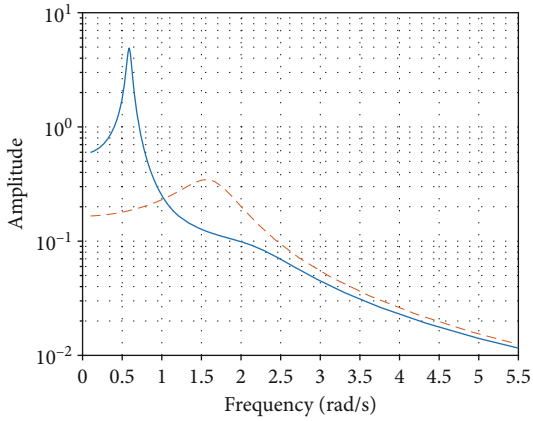

Figure 9: The frequency response for the original system $H_{3,3}$ (solid line) and modified system $H_{3,3}$ (dotted line).

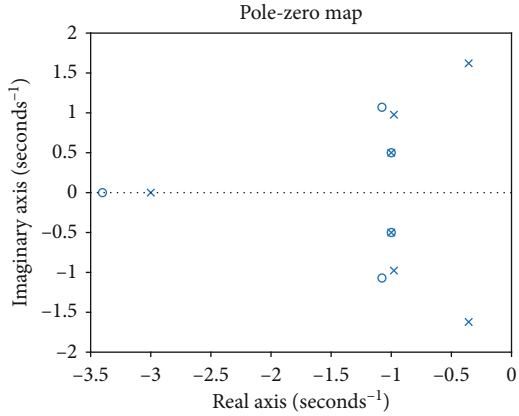

Figure 10: The pole-zero map for the modified system $H_{3,3}$.

results indicate that the proposed method is generally effective. The proposed method in this paper can be utilized to improve performance and reliability on robotic systems such as flexible robots, robot arms, and intelligent vehicles. In future work, the proposed method will be expanded to handle vibration control tasks for nonlinear systems with multi inputs and outputs.

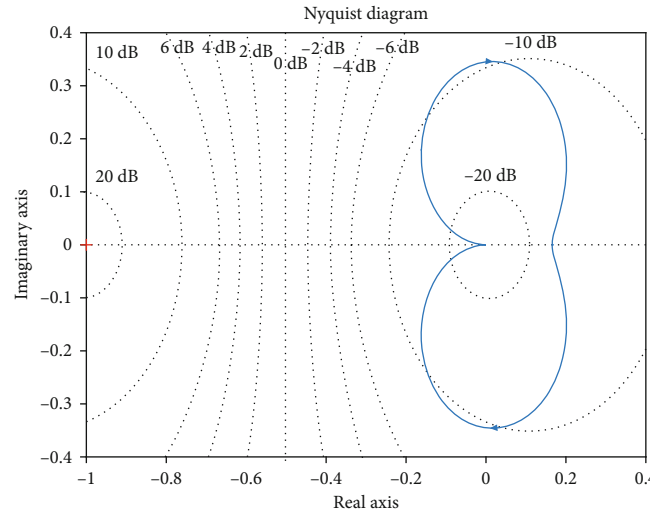

Figure 11: The Nyquist curve for the modified system $H_{3,3}$.

Data Availability

No data was used to support this study.

Conflicts of Interest

The authors declare that there is no conflict of interest regarding the publication of this paper.

Acknowledgments

This work is supported by the Key Science and Technology Research Project of Chongqing (cstc2018jszx-cyztzxX0032).

References

[1] J. J. Lima, J. M. Balthazar, R. T. Rocha et al., "On positioning and vibration control application to robotic manipulators with a nonideal load carrying," *Shock and Vibration*, vol. 2019, Article ID 5408519, 14 pages, 2019.

[2] Y. Chang, Y. Wang, F. E. Alsaadi, and G. Zong, "Adaptive fuzzy output-feedback tracking control for switched stochastic pure-feedback nonlinear *systems*," *International Journal of Adaptive Control and Signal Processing*, vol. 33, no. 10, pp. 1567–1582, 2019.

[3] Y. Wang, Y. Chang, A. F. Alkhateeb, and N. D. Alotaibi, "Adaptive fuzzy output-feedback tracking control for switched nonstrict-feedback nonlinear systems with prescribed performance," *Circuits, Systems, and Signal Processing*, vol. 39, 2020.

[4] L. Ma, N. Xu, X. Huo, and X. Zhao, "Adaptive finite-time output-feedback control design for switched pure-feedback nonlinear systems with average dwell time," *Nonlinear Analysis: Hybrid Systems*, vol. 37, p. 100908, 2020.

[5] X. H. Chang, Y. Liu, and M. Shen, "Resilient control design for lateral motion regulation of intelligent vehicle," *IEEE/ASME*

Transactions on Mechatronics, vol. 24, no. 6, pp. 2488–2497, 2019.

[6] L. Ma, G. Zong, X. Zhao, and X. Huo, "Observed-based adaptive finite-time tracking control for a class of nonstrict-feedback nonlinear systems with input saturation," *Journal of the Franklin Institute*, 2019.

[7] R. Mou, L. Hou, Y. Jiang, Y. Zhao, and Y. Wei, "Study of automobile suspension system vibration characteristics based on the adaptive control method," *International Journal of Acoustics & Vibration*, vol. 20, no. 2, pp. 101–106, 2015.

[8] J. de Jesus Rubio, P. Cruz, L. A. Paramo, J. A. Meda, D. Mujica, and R. S. Ortigoza, "PID anti-vibration control of a robotic arm," *IEEE Latin America Transactions*, vol. 14, no. 7, pp. 3144–3150, 2016.

[9] Y. Sekhar and C. Vinothkumar, *Ieee. Development of a Lab View Based Controller for Active Vibration Control of Panel Structures Using Piezo-Electric Wafers*, Ieee, New York, 2016.

[10] M. L. Xia and S. Li, "A combined approach for active vibration control of fluid-loaded structures using the receptance method," *Archive of Applied Mechanics*, vol. 88, no. 10, pp. 1683–1694, 2018.

[11] Y. M. Ram and J. E. Mottershead, "Receptance method in active vibration control," *AIAA Journal*, vol. 45, no. 3, pp. 562–567, 2007.

[12] J. E. Mottershead, M. G. Tehrani, and Y. M. Ram, "Assignment of eigenvalue sensitivities from receptance measurements," *Mechanical Systems and Signal Processing*, vol. 23, no. 6, pp. 1931–1939, 2009.

[13] J. F. Zhang, H. J. Ouyang, and J. Yang, "Partial eigenstructure assignment for undamped vibration systems using acceleration and displacement feedback," *Journal of Sound and Vibration*, vol. 333, no. 1, pp. 1–12, 2014.

[14] H. Ouyang, "Pole assignment of friction-induced vibration for stabilisation through state-feedback control," *Journal of Sound and Vibration*, vol. 329, no. 11, pp. 1985–1991, 2010.

[15] S. M. Gharghory and A. E. Ebrahim, "Self-adaptive firefly algorithm with pole zero cancellation method for controlling SMIB power system," *International Journal of Computational Intelligence and Applications*, vol. 18, no. 2, p. 1950013, 2019.

[16] A. S. Chopade, S. W. Khubalkar, A. S. Junghare, M. V. Aware, and S. Das, "Design and implementation of digital fractional order PID controller using optimal pole-zero approximation method for magnetic levitation system," *IEEE/CAA Journal of Automatica Sinica*, vol. 5, no. 5, pp. 977–989, 2018.

[17] X. Fengxia, Z. Xuejie, S. Xiaohui, and W. Shanshan, "Composite control of RBF neural network and PD for nonlinear dynamic plants using U-model," *Journal of Intelligent Fuzzy Systems*, vol. 35, no. 1, pp. 565–575, 2018.

[18] R. Song and S. Chen, "A self-tuning proportional-integral-derivative-based temperature control method for draw-texturing-yarn machine," *Mathematical Problems in Engineering*, vol. 2017, Article ID 1864321, 17 pages, 2017.

[19] L. E. Ciotirca, O. Bernal, J. Enjalbert et al., "New stability method of a multirate controller for a three-axis high-Q MEMS accelerometer with simultaneous electrostatic damping," *IEEE Sensors Journal*, vol. 18, no. 15, pp. 6106–6114, 2018.

[20] R. Samin, M. G. Tehrani, and J. E. Mottershead, "Active vibration suppression by the receptance method: partial pole placement, robustness and experiments," in *Vibration Problems Icovp 2011*, J. Naprstek, J. Horacek, M. Okrouhlik, B. Marvalova, F. Verhulst, and J. T. Sawicki, Eds., vol. 139 of Springer Proceedings in Physics, pp. 371–377, Springer-Verlag Berlin, Berlin, 2011.

[21] J. Y. Ishihara and M. H. Terra, "On the Lyapunov theorem for singular systems," *IEEE Transactions on Automatic Control*, vol. 47, no. 11, pp. 1926–1930, 2002.

[22] Y. M. Ram, "Pole-zero assignment of vibratory systems by state feedback control," *Journal of Vibration and Control*, vol. 4, no. 2, pp. 145–165, 2016.